LAPP-EXP 98-06
September 1998

EXPERIMENTAL ASPECTS OF QCD IN e^+e^- COLLISIONS

D. DUCHESNEAU

**LAPP, IN2P3-CNRS, Chemin de Bellevue, BP110,
F-74941, Annecy-le-Vieux**

abstract

A review of the most recent experimental tests of QCD in e^+e^- annihilation is given. It covers the following topics: determination of α_s from event shapes, improved tests of flavour independence of α_s, studies of heavy quark mass effects, improved understanding of quark and gluon jet differences and several aspects of fragmentation studies.

Plenary talk given at the $XXIX^{th}$ International Conference on High Energy Physics, ICHEP'98,
23-29 july 1998, Vanvouver, Canada

EXPERIMENTAL ASPECTS OF QCD IN e^+e^- COLLISIONS

D. DUCHESNEAU

LAPP,IN2P3-CNRS, Chemin de Bellevue, BP110,
F-74941, Annecy-le-Vieux, France
E-mail: duchesneau@lapp.in2p3.fr

A review of the most recent experimental tests of QCD in e^+e^- annihilation is given. It covers the following topics: determination of α_s from event shapes, improved tests of flavour independence of α_s, studies of heavy quark mass effects, improved understanding of quark and gluon jet differences and several aspects of fragmentation studies.

1 Introduction

The study of hadronic events produced in e^+e^- annihilation has made a major contribution to establishing QCD as the theory of the strong interaction. This is partly due to the fact that e^+e^- interactions offer a very clean environment to study hadron production. In this process all the hadronic activity is limited to the final state, there is no contamination from beam remnants, and apart from initial and final state radiation the hadronic center of mass energy is well defined. At sufficiently high energy the primary partons (quarks or gluons) produced in the e^+e^- annihilation process start to form collimated clusters of particles (jets) clearly signing their existence. Thus the first evidence for the existence of the quark was the observation of two-jet structure in hadronic events produced in e^+e^- collisions at SPEAR [1], and the observation of the first three-jet event at PETRA in 1979 gave the first evidence for the existence of the gluon [2]. A short historical review can be found in Ref. 3. It is believed that hadron jets reflect the properties of the underlying quarks and gluons. The study of the jet structure of hadronic events is then a powerful tool to probe the parton dynamics, allowing measurements of the strong coupling constant α_s and tests of perturbative QCD predictions. In addition careful study of the particle distributions within the jets gives valuable information to investigate the transition between the perturbative and the so called non-perturbative regime of the hadron production in which the colored partons transform into colorless hadrons.

For more than 20 years very active work has been done at various e^+e^- colliders to perform quantitative tests of QCD. Some detailed reviews of these studies can be found e.g. in Ref. 4. This research field is still very active and this paper reviews most of the new results from QCD studies in e^+e^- collisions which have been submitted to this conference. The outline is as follows: after a brief overview of the theoretical and experimental frameworks, new results from QCD studies at high energies (LEP2) and consistency checks of the theory are discussed in section 4. New determinations of α_s from event shape observables are shown in section 5. The QCD studies, including heavy quark mass effects in 3-jet events, allowing improved tests of flavour independence of α_s are discussed in section 7. In section 8 4-jet production is mentioned with new measurements of the gluon splitting process into heavy quarks. In section 9 results on particle multiplicity and momentum spectra at various energies are shown and compared with QCD predictions. New precise studies of the properties of quark and gluon jets are reviewed in section 10. Finally, before summarizing, results on particle production and correlation studies are briefly discussed in section 11.

2 Theoretical framework

From the theoretical point of view the process of hadron production from a quark-antiquark pair in e^+e^- annihilations may be seen as composed of two different regimes governed by the strong interactions and referred to as perturbative and non-perturbative phases. Asymptotic freedom, which is a fundamental property of QCD, tells us that the strong coupling constant decreases with energy such that calculation techniques based on perturbation theory may be applied to describe quark and gluon production with high momentum transfers. This defines the first regime corresponding to a parton cascade where primary quarks split into further partons down to a certain energy scale ($\approx$ 1 GeV) where perturbative techniques cease to be valid. The main perturbative calculations available today to describe the hadronic event structure at parton level are:

- $\mathcal{O}(\alpha_s^2)$ calculations of event shape variables [5] for which the most recent developments have been improved $\mathcal{O}(\alpha_s^2)$ calculations including the event orientation [6] and complete calculations for massive quarks of several event shape variables [7,8,9].

- Improved calculations incorporating the resummation of leading and next-to-leading logarithmic

Table 1: Main characteristics of the highest e^+e^- colliders.

	$\sqrt{s}$ (GeV)	$\mathcal{L}$ (pb^{-1}) /expt	# of $q\overline{q}$ /expt	dates
PETRA/PEP	14-46	200	40K	1978→1990
TRISTAN	50-64	300	40K	1987→1995
SLC	91.2	15	500K	1993→1998
LEP1	91.2	125	4000K	1989→1995
LEP2	130-189	125	3K	1995→1998

terms [10] matched to $\mathcal{O}(\alpha_s^2)$ results for several event shape variables

- New $\mathcal{O}(\alpha_s^3)$ calculation (full 1-loop) of 4 parton states [11]
- Analytical calculations based on several leading log approximations [12]

In order to relate the parton level fixed order calculations to final state hadrons one method is to use phenomenological models describing the non-perturbative transition phase. These models are included in the commonly used QCD models. The most successful approach is the Lund string fragmentation implemented in JETSET model. The cluster model implemented in HERWIG generator is also widely used, however with less success, in e^+e^- studies.
Another approach which seems to be promising consists of describing the non-perturbative effects analytically by means of power corrections. These corrections have been calculated for mean values and differential distributions of some e^+e^- event shape observables [13].
Finally, in the case of analytical calculations of inclusive quantities the hypothesis of Local Parton Hadron Duality (LPHD) [14] is usually invoked. It suggests that the calculated parton distributions can be compared directly to the measured hadron distributions.

3 Experimental framework

Most of the new results presented at this conference come from the LEP and SLC colliders. Table 1 summarises the main characteristics of the highest e^+e^- colliders since 1978. One can see that the largest samples of hadronic events have been obtained at LEP and SLC running on the Z pole ($\sqrt{s}\approx$91.2 GeV). They correspond to about 0.5 M hadronic events for SLD experiment and about 4M events per LEP experiment (ALEPH, DELPHI, L3 and OPAL).

Due to the large hadron cross section, negligible background from other processes and a strong suppression of initial state radiation the Z resonance offers unique conditions to do very detailed studies of hadronic event structure and precise tests of perturbative QCD.

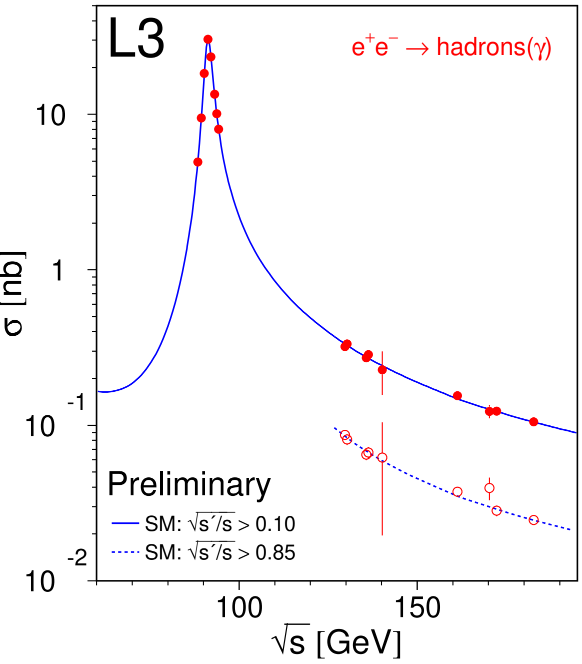

Figure 1: Hadron cross section measured by L3 from 91 GeV to 183 GeV.

Since 1995 the LEP machine has increased the beam energies in several steps, corresponding to the LEP2 program. Thus the average center of mass energy obtained was 133 GeV, 161 GeV, 172 GeV, 183 GeV and this year LEP is running at 189 GeV. The hadron cross section measured by L3 up to 183 GeV is shown in figure 1 as a function of $\sqrt{s}$. One can see that, compared to 91 GeV runs, the experimental situation at LEP2 is not so ideal for QCD studies. The cross section is much lower and a large fraction of the events correspond to hard initial state radiation bringing down the effective hadronic center of mass energy $\sqrt{s'}$ to the Z pole. When these events with hard ISR are rejected the data samples have typically a few hundred to a few thousand hadronic events per energy point. In addition to this potential limitation, the dominant background above 161 GeV comes from W pairs decaying into 4 quarks. Part of this background is rejected using topological identification and the remaining contamination is subtracted according to model predictions. This is treated as a possible source of systematic error for all the studies at LEP2.

3.1 Flavour tagging

The very precise microvertex detectors existing in the tracking systems of SLD and of the 4 LEP experiments have allowed new QCD flavour dependent studies to be

performed these last years with the large data samples collected at 91 GeV. Typically light quark (uds) and b quark jets are tagged with purities ranging between 80% and 98% while c-quark jets are identified with purities between 55% and 64%.
Applying quark flavour tagging to 3-jet events offers a clean method to tag gluon initiated jets reaching purities up to 94% allowing precise studies of gluon jet properties. Several new results reviewed in this report are based on these tagging capabilities.

4 Global event properties and tests of QCD models

The jet structure of hadronic events can be analysed using global event shape variables which are sensitive to gluon radiation. As already mentioned QCD models are used to compute hadronization corrections and we need to have reliable models working at various energies. At LEP2 consistency checks are important due to the intensive use of QCD models in most research fields, especially W pair production studies and new particle searches which are the main LEP phase 2 issues and for which QCD events are the main background. All the known models have been tuned and tested in great detail on the Z pole at SLC and LEP [15]. Because these models are based on first QCD principles, an important test is to check the predicted energy evolution of the shape distributions using the same Monte Carlo parameter values. This energy dependence arises mainly from 2 sources: the logarithmic energy scale dependence of α_s and the power law behaviour of the non-perturbative effects. LEP2 is a good place to check the consistency of QCD predictions. For illustration figure 2 shows the thrust distribution T as measured by L3 at $\sqrt{s}$=183 GeV compared to PYTHIA, HERWIG, ARIADNE and COJETS Monte Carlo models tuned at 91 GeV. The agreement is quite satisfactory at the distribution level and similar conclusions have been drawn at 183 GeV by the 4 LEP collaborations for variables describing the global event structure [16,17,18,19].

The energy dependence is clearly seen when studying the mean values of the event shape variable. Figure 3 shows the mean thrust value as a function of the e^+e^- center of mass energies measured from 14 GeV to 189 GeV [18]. Also shown are the energy dependences of these quantities as predicted by several QCD Monte Carlo models with constant parameter values over the full energy range. These models use different approaches to describe the perturbative and non perturbative phases of QCD evolution. All parton shower models are in agreement with the present measurements of mean event shape variables and are able to take into account properly the main sources of energy dependence.

In addition to event shapes jet rates are powerful

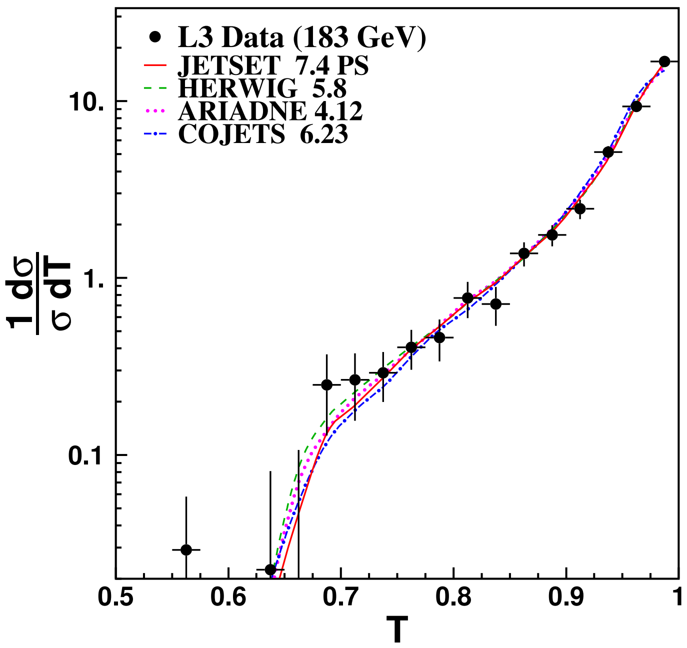

Figure 2: Thrust distribution measured by L3 at $\sqrt{s}$ = 183 GeV compared to various QCD models

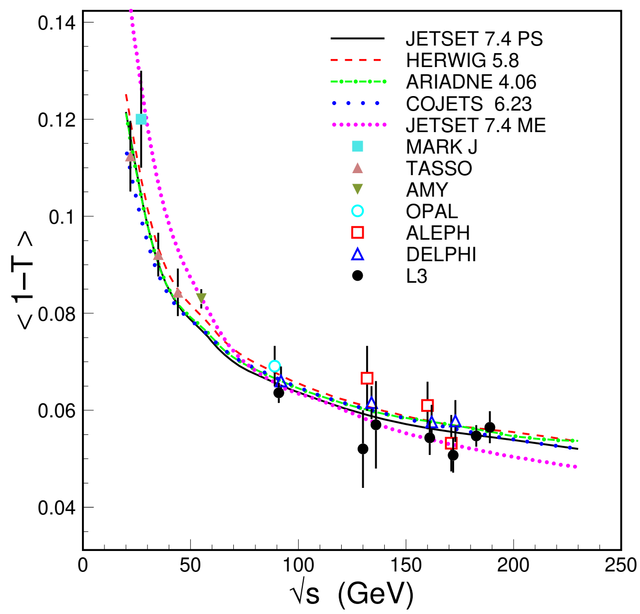

Figure 3: Mean thrust value as a function of the CM energy.

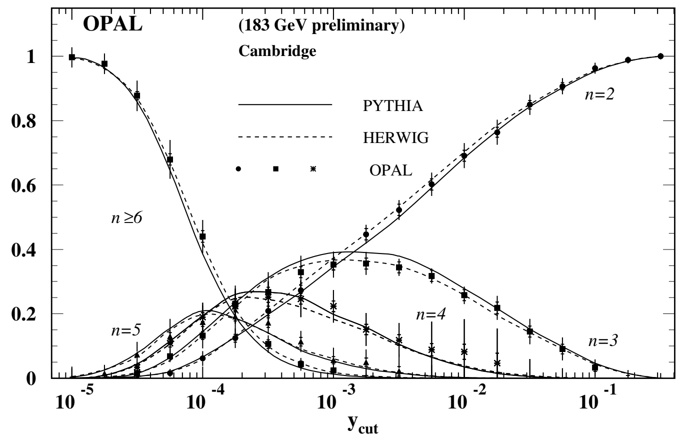

Figure 4: Measured fraction of 2-, 3-, 4-, 5- and more jet events as a function of y_{cut} for the Cambridge jet finding scheme.

tools to investigate the hadronic event structure. It gives direct information about hard parton configurations. There are several jet clustering algorithms which differ in their combination scheme and object pairing. At LEP and SLC the most widely used are JADE and Durham algorithms. Recently a new clustering method called the "Cambridge Algorithm" [20] has been introduced. It is a modified version of Durham designed to reduce non-perturbative corrections and to provide better resolution of jet substructure. The main difference with the conventional method is that the ordering variable is different from the test variable and there is a freezing of soft resolved objects in the clustering sequence. A discussion of this algorithm and a comparison of its performance with the Durham one is given in Ref. 21. From this comparative study it is not obvious that Cambridge algorithm provides smaller hadronization corrections than Durham algorithm. Figure 4 shows the OPAL measurement at 183 GeV of jet rates obtained with this new jet algorithm[19]. The parton shower models PYTHIA and HERWIG provide a good description of the measured jet rates up to very large number of jets (corresponding to subjets at very small resolution parameter value y_{cut}).

5 Determination of α_s from event shapes

The strong coupling constant α_s is the only free parameter of QCD. The theory does not predict a fixed value for this constant but only its energy behaviour known as "asymptotic freedom". Thus, the experimental observation of the running of α_s(Q) according to QCD is a fundamental test of the underlying non-abelian gauge theory. In e^+e^- annihilations several methods exist to determine α_s which are based on the fact that, experimentally, α_s is not directly observable. It is extracted from physical quantities sensitive to QCD effects written in form of perturbative predictions. The commonly used quantities for which fixed order perturbative predictions exist are:

- The ratio of the hadronic and leptonic partial widths of the Z boson (R_l) known to $\mathcal{O}(\alpha_s^3)$ [22]
- The total hadronic width of the τ lepton (R_τ) and the spectral moments of the hadron mass distribution which have been calculated to $\mathcal{O}(\alpha_s^3)$ [23]
- Several event shape variables calculated up to $\mathcal{O}(\alpha_s^2)$ [5]

Most of the new contributions on α_s determination submitted at this conference concern event shape variables and are discussed in this section. The new results from the other methods are briefly reviewed in section 6.
The event shape observables are sensitive to the amount of hard gluon radiation and offer the most direct way to measure α_s while the fully inclusive quantities like R_l are sensitive to α_s only through radiative corrections and require very precise measurements.

5.1 *Fixed order calculation*

To be calculable in perturbative QCD an observable should be infrared and collinear safe. The observables built from linear sums of momenta like thrust, heavy jet mass etc... fulfill these requirements and the event shape differential distribution calculated to second order in α_s at parton level is usually given by [5]:

$$\frac{1}{\sigma}\frac{\mathrm{d}\sigma}{\mathrm{dy}} = \frac{\alpha_\mathrm{s}(\mu)}{2\pi}\mathrm{A(y)} + \left(\frac{\alpha_\mathrm{s}(\mu)}{2\pi}\right)^2\left[\mathrm{B(y)} + 2\pi\beta_\circ\ln(\mu^2/\mathrm{s})\mathrm{A(y)}\right] \quad (1)$$

where μ is the renormalisation scale at which α_s is evaluated. At first order, these event shape variables are proportional to α_s, giving a strong sensitivity to α_s. One of the advantages of this method for evaluating α_s is that the $\mathcal{O}(\alpha_s^2)$ coefficients A(y) and B(y) have been calculated for more than 15 variables.

However the main limitation coming from the fixed order calculation is the renormalisation scale and renormalisation scheme dependence due to the power series truncation. This leads to large uncertainties coming from the unknown missing higher order terms of the expansion. This μ dependence should disappear when the expression is computed to all orders. The difficulty resides in determining the effect of the renormalisation scale uncertainty and in choosing the right scale for the calculation to be valid. Intuitively the physical scale should

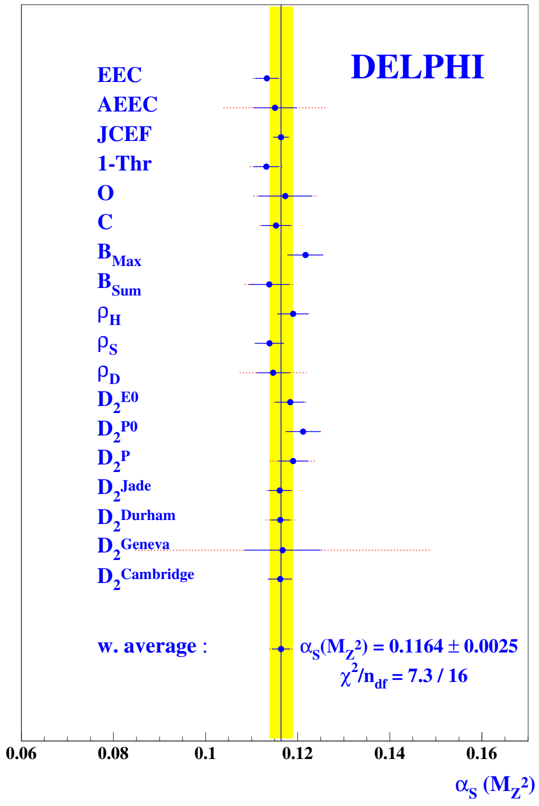

Figure 5: Results of the fits of the 18 event shape distributions to $\mathcal{O}(\alpha_s^2)$ calculations together with their weighted average.

be the e^+e^- CM energy $\sqrt{s}$ but first studies at LEP and SLD have shown that to achieve good fits with second order calculations to the measured distributions the scale should be much smaller than the physical scale $\sqrt{s} = M_Z$. The errors attributed to the scale uncertainty were obtained from the variation of the results when the scale was changed by a large factor around the nominal value taken equal for all the variables.

This problem of scale definition has been reassessed by a new DELPHI measurement presented at this conference where $\mathcal{O}(\alpha_s^2)$ calculations including event orientation have been fitted for 18 event shape variables measured with 1.5 M hadronic events at LEP1 [24]. The renormalisation scale ambiguity has been treated by doing a combined fit of α_s and the μ scale for each variable. The 18 values of α_s are shown in figure 5.

For these experimentally optimized scale values, ranging from 0.003 for thrust to 6.02 for Geneva algorithm, very consistent values of α_s have been obtained with, in each case, a weak dependence on μ providing small renormalisation scale uncertainty. The weighted average taking into account correlations between the observables yields the value: $\alpha_s(m_Z) = 0.1164 \pm 0.0025$ with a quite small error. Theoretically motivated "optimized" scales [25] give results in agreement with the quoted α_s value. Experimental optimisation of scales was already proposed in 1989 [26] but did not reach a consensus at that time between experimentalists and theorists and a more conservative approach was used to assess the μ scale ambiguity with fixed order calculations. In the future this experimental procedure should be the focus of particular attention. The use of resummed calculations available since 1992 has provided a partial solution to the μ scale ambiguity and is giving satisfactory results for the measurement at various energies.

5.2 Resummed calculations

In the fixed order calculation there are terms corresponding to soft and collinear radiation, dominating the 2-jet region. These logarithmically enhanced terms spoil the convergence of the fixed order expansion and higher order terms are needed to have a reliable calculation in regions where this multiple gluon emission dominates. For certain variables it is possible to isolate the Leading-Log and Next-to-Leading-log terms of infrared origin in every order of the perturbation series and to sum them up in the form of an exponential. These calculations which do not include heavy quark mass effects are performed at parton level for a few observables [10]. When matched properly to fixed order calculations, this gives a quite reliable QCD prediction (O(α_s^2)+NLLA) over a wider range of values of the event shape variables. This is an advantage when the data samples are small as at LEP2 energies. A very interesting advantage of the resummed calculation is the reduction of the renormalisation scale uncertainty compared to fixed order and the fact that a unique value of μ gives consistent results for various variables.

Measurements of the strong coupling constant at high energies have been performed by ALEPH, DELPHI, L3 and OPAL by fitting combined O(α_s^2)+NLLA QCD calculations to a certain number of corrected event shape distributions for which the theoretical descriptions are the most complete. These are the thrust (T), scaled heavy jet mass (ρ), total and wide jet broadenings (B_T and B_W), C-parameter and differential 2-jet rate. As an example table 2 summarises the α_s values obtained by the 4 LEP experiments at 183 GeV. In the case of ALEPH [27] and OPAL [19] the second error correspond to the experimental systematic and theoretical errors while L3 [18] and DELPHI [28] include the systematic error in the first error. The variables used are given in the last column.

It is interesting to mention that all the experiments use different variables, different fit ranges and different averaging method of the variables to obtain their values.

Table 2: α_s values obtained at 183 GeV by fitting event shape distributions with resummed fixed order calculations.

	α_s(183 GeV)					fit variable
ALEPH	0.1093	$\pm$	0.0020(stat)	$\pm$	0.0036(syst)	T,ρ,B_w,C,$-lny_3$
DELPHI	0.1127	$\pm$	0.0059(exp)	$\pm$	0.0048(th)	T,ρ
L3	0.1086	$\pm$	0.0026(exp)	$\pm$	0.0054(th)	T,ρ,B_w, B_t
OPAL	0.104	$\pm$	0.003(stat)	$\pm$	0.005(syst)	T,M_H,B_w, B_t, D_2

Despite these differences, the values are very consistent between the 4 experiments. To compare the analytical calculations with the experimental distributions, the effects of hadronization and decays are usually corrected using Monte Carlo programs.

5.3 α_s using power corrections

DELPHI uses a method independent of fragmentation model corrections to determine α_s from the energy dependence of the mean thrust and heavy jet mass [28]. Instead of using hadronization models to determine the non-perturbative corrections to the analytical calculations power correction terms are applied.

The mean value of an event shape variable f can be written in the form:

$$\langle f \rangle = \frac{1}{\sigma_{tot}} \int f \frac{d\sigma}{df} df = \langle f_{pert} \rangle + \langle f_{pow} \rangle \qquad (2)$$

where $\langle f_{pert} \rangle$ is the O(α_s^2) expression for the event shape distribution and $\langle f_{pow} \rangle$ is a power correction term taking into account the hadronization effect. Following the prescription given in Ref. 13 the power corrections have the general form:

$$\langle f_{pow} \rangle = a_f \frac{4C_F}{\pi^2} M \frac{\mu_I}{E_{cm}} [\alpha_0(\mu_I) - \alpha_s(\mu) - \left(b_0 \log \frac{\mu^2}{\mu_I^2} + \frac{K}{2\pi} + 2b_0 \right) \alpha_s^2(\mu)] \qquad (3)$$

where α_0 is a non-perturbative parameter accounting for the contributions to the event shape below and infrared maching scale μ_I and M is the Milan factor to take into account 2-loop corrections. Beside α_s, α_0 is the only free parameter. The coefficient a_f has been calculated for thrust, C-parameter, heavy jet mass and total and wide jet broadening variables. Figure 6 shows the measured mean values of thrust, $< 1 - T >$, and scaled heavy jet mass, $< M_h^2/E_{vis}^2 >$, as a function of the centre of mass energy measured from 14 GeV to 183 GeV.

DELPHI has used the previous ansatz to determine α_s from mean thrust and mean heavy jet mass. α_0 is first obtained by doing a combined fit of α_s and α_0 to the large set of measurements from 14 GeV to 91 GeV adding the

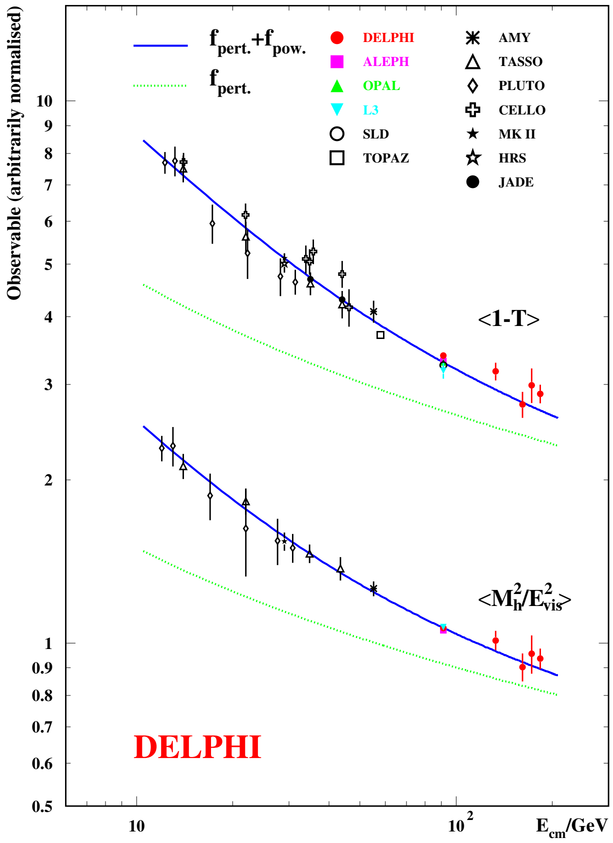

Figure 6: Mean values of thrust and heavy jet mass as a function of e^+e^- CM energy. The solid curve is the result of a fit using O(α_s^2)+power corrections while the dashed line is the O(α_s^2) prediction.

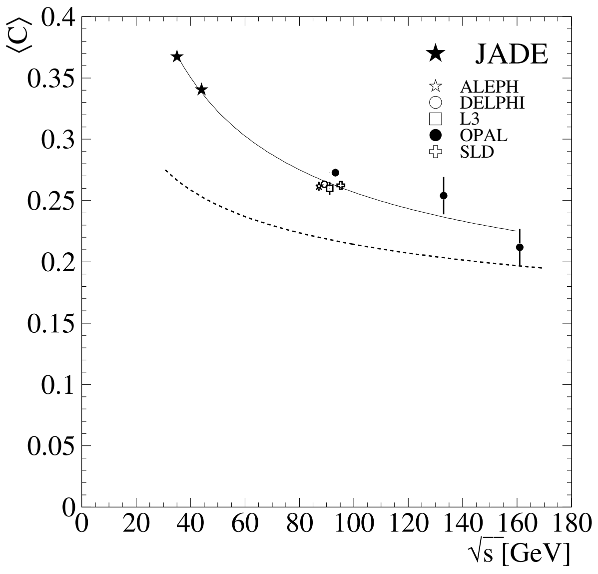

Figure 7: Same as figure 6 but for the mean value of the C-parameter.

DELPHI measurements above 91 GeV. The result of the fit is shown as the solid curve in Fig. 6. α_0 is found to be about 0.5 as expected but seems not to have a universal value for all the observables as is sometimes assumed. The disagreement between the 2 values is about 10%. After having fixed α_0 the α_s values corresponding to the high energy points are calculated from Eq. (3) giving at 183 GeV:
$\alpha_s(183 \text{ GeV}) = 0.1125 \pm 0.0056 \text{ (exp)} \pm 0.0035 \text{ (scale)}$. This value is clearly in agreement with the values shown in table 2 but with the experimental error larger than the theoretical error estimated from the renormalization scale uncertainty and from the variation of μ_I.

In a recent reanalysis of the JADE data [29] the C-parameter and the broadening variables have been measured at 35 GeV and 44 GeV. Using these new measurements a similar analysis based on power corrections as described above has been repeated and the universality of α_0 has been found only at a level of 30%. The α_0 values obtained from $< 1 - T >$ and $< M_h^2/E_{vis}^2 >$ are compatible with the ones found by DELPHI. The α_s values obtained from $< C >$, $< B_T >$ and $< B_W >$ are consistent among each other.

Figure 7 shows the measured mean values of the C-parameter as a function of $\sqrt{s}$. The JADE points provide the only measurements below 91 GeV necessary to accurately determine the power corrections.

ALEPH has applied directly the power corrections to the event shape distributions of thrust and C-parameter to determine α_s [27]. These corrections should correspond to a shift of the whole distribution which can be expressed

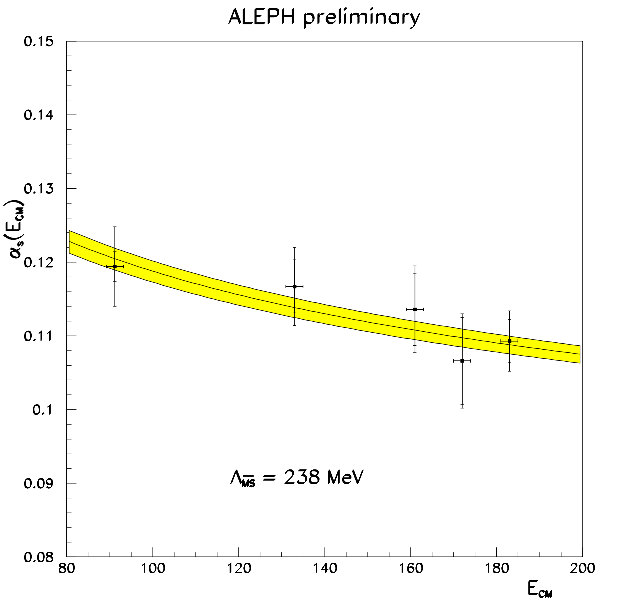

Figure 8: Measured values of α_s by ALEPH from a combined analysis of 5 event shape variables. The curve corresponds to the 3-loop QCD prediction.

in a similar form to the mean values. Fitting the distributions α_0 values are obtained compatible between the 2 observables giving an average value of:

$$\alpha_0(2 \text{ GeV}) = 0.451 \pm 0.003 \text{ (stat)} \pm 0.065 \text{ (syst)}.$$

Using this value a combined fit to the C and T distributions gives:

$$\alpha_s\ (m_Z) = 0.1168 \pm 0.0003 \text{ (stat)} \pm 0.0048 \text{ (syst)}.$$

In the ALEPH paper it is reported that this procedure doesn't work properly in the case of the heavy jet mass distribution.

5.4 Running of α_s

Each of the 4 LEP experiments has derived α_s at several energies using the same experimental technique and the same calculation, allowing them to study the energy dependence of α_s using only identified uncorrelated errors. They all have results which are compatible with the energy evolution predicted by QCD but the errors are such that it is difficult to be sensitive to any deviation with the actual precision. Figure 8 shows the α_s values measured by ALEPH from 91 GeV to 183 GeV [27] using the 5 variables given in table 2 with the resummed fixed order calculation. The inner error bars correspond to the uncorrelated component which is used to extract $\alpha_s(m_Z)$ from a simultaneous fit of the 4 measurements above the Z assuming the 3-loop QCD evolution equation for α_s. This gives:

$$\alpha_s\ (m_Z) = 0.1217 \pm 0.0017 \text{ (stat)} \pm 0.0044 \text{ (syst)}.$$

L3 has used a wider lever arm to study the energy

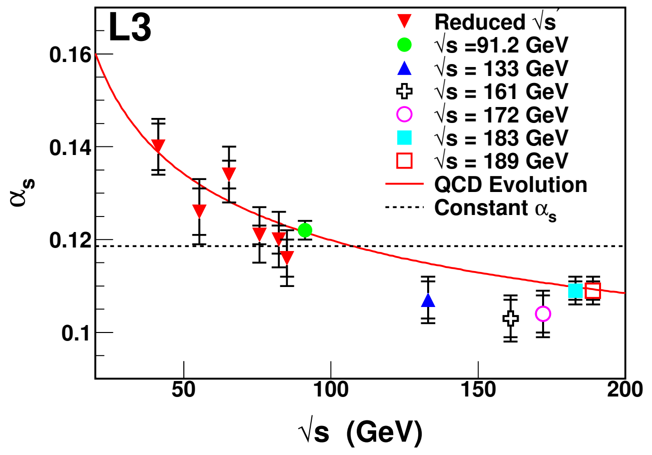

Figure 9: Measured values of α_s by L3 from event shape distributions as a function of the CM energy.

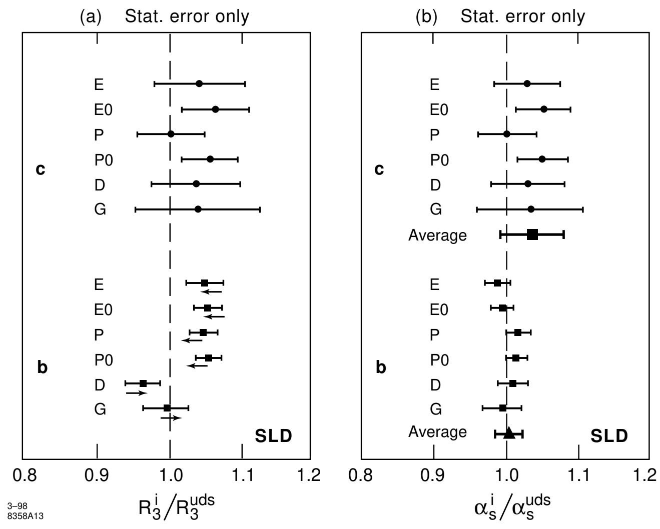

Figure 10: (a) The measured 3-jet rate ratios R_3^i/R_3^{uds} and (b) the corresponding translated ratios $\alpha_s^i/\alpha_s^{uds}$ where i = c, b. In (b) the weighted average over the six jet algorithms is also shown.

dependence of α_s. Radiative events measured on the Z pole are used to determine six α_s values between 30 GeV and 88 GeV. These measurements are shown in figure 9 together with the higher energy values obtained up to 189 GeV. The errors are only experimental. A fit to the QCD evolution equation gives [18]:

$\alpha_s\ (m_Z) = 0.1216 \pm 0.0017\ (\text{exp}) \pm 0.0058\ (\text{th})$.

with a χ^2 of 16.9 for 10 degrees of freedom corresponding to a confidence level of 0.076. The constant α_s hypothesis gives a χ^2 of 91.4 and is clearly ruled out.

6 Other α_s determinations

From the theoretical point of view the most reliable determination of α_s comes from the radiative QCD correction to the hadronic width of the Z. The latest value extracted from R_l is [30]:

$\alpha_s\ (m_Z) = 0.124 \pm 0.004\ (\text{exp}) \pm 0.002\ (M_H)$.

The most precise determination of α_s in e^+e^- annihilation is from the detailed studies of the vector and axial-vector spectral functions of hadronic τ decays from ALEPH [31] and OPAL [32]. The combined result from these 2 new measurements is [33]:

$\alpha_s\ (m_\tau) = 0.339 \pm 0.021$ which translates into

$\alpha_s\ (m_Z) = 0.120 \pm 0.003$.

No new result has been reported on the determination of α_s from scaling violation in fragmentation functions. A discussion about our current knowledge of α_s is given in Ref. 34.

7 Flavour independence of α_s and heavy quark mass effects

QCD predicts the strong coupling constant to be independent of the quark flavour. Testing this assumption is an important test of QCD and any deviation should be a sign for new physics. This flavour independence is tested by measuring α_s for different flavour tagged hadronic event samples. SLD has presented a measurement of the 3-jet rate measured with six different jet algorithms, for b and c events [35]. The b and c samples have been obtained on the basis of the reconstructed mass of long lived heavy hadron decay vertices and charged track impact parameter.

Figure 10(a) shows the ratio of 3-jet rate for b and c quarks to the 3-jet rate for uds quarks measured with the six jet algorithms. In the case of b this ratio is significantly different from 1 and has a large spread among the six algorithms. These differences are predicted by the NLO calculations including quark mass effects [8]. The arrows in Fig. 10(a) indicate the range of the theoretical prediction for R_3^b/R_3^{uds} for values of $m_b(m_Z)$ between 2.5 and 3.5 GeV/c^2. With the present experimental accuracy the mass effects for the c quark which should be of the order of 1% are not seen. Figure 10(b) shows the ratios $\alpha_s^c/\alpha_s^{uds}$ and $\alpha_s^b/\alpha_s^{uds}$ extracted from the 3 jet rate ratios with the 6 jet algorithms using the NLO prediction. Combining the results from the different jet algorithm gives:

$$\frac{\alpha_s^c}{\alpha_s^{uds}} = 1.036 \pm 0.043\,(stat)^{+0.041}_{-0.045}\,(syst)^{+0.020}_{-0.018}\,(th) \quad (4)$$

$$\frac{\alpha_s^b}{\alpha_s^{uds}} = 1.004 \pm 0.018\,(stat)^{+0.026}_{-0.031}\,(syst)^{+0.018}_{-0.029}\,(th) \quad (5)$$

These results are compatible with the flavour independence of α_s.

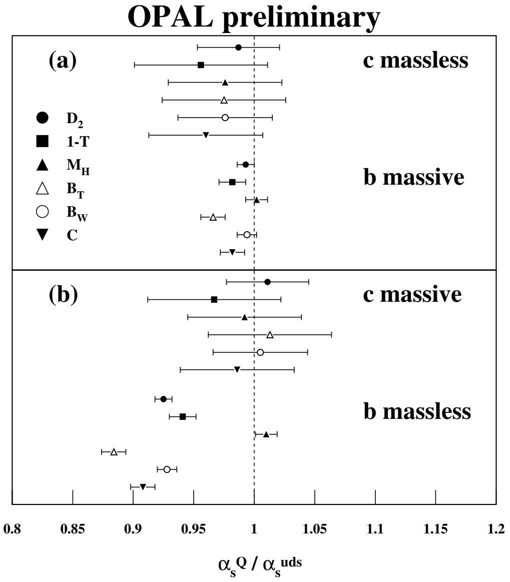

Figure 11: The ratios $\alpha_s^c/\alpha_s^{uds}$ and $\alpha_s^b/\alpha_s^{uds}$ determined in two different ways as described in the text. The errors shown are only statistical.

OPAL has also performed an improved test of the flavour independence of α_s [36]. A quite different flavour tagging technique is used for the c quark based on $D^{*\pm}$ reconstruction giving similar purity but smaller efficiency. For each tagged sample six event shape variables are measured: thrust (T), scaled heavy jet mass (ρ=M_H^2/E_{vis}^2), total jet broadening (B_T), wide jet broadening(B_W), differential 2-jet rate (D_2) and C-parameter. Knowing the different flavour purities of each sample the ratios $\alpha_s^c/\alpha_s^{uds}$ and $\alpha_s^b/\alpha_s^{uds}$ are extracted by fitting the NLO QCD predictions to these distributions taking into account b and c quark mass effects given by the calculation of Ref. 9. Figure 11 shows the results of the fit for the 6 event shape variables for 2 different conditions:(a) considering c massless and b massive and (b) considering c massive and b massless. The errors shown are only statistical. Thus the effect of the b mass is clearly seen and to get consistent results from the different observables the calculation should include the b mass.

Combining the results from the 6 event shape variables gives:

$$\frac{\alpha_s^c}{\alpha_s^{uds}} = 1.002 \pm 0.017\,(stat) \pm 0.025\,(syst) \pm 0.009\,(th) \tag{6}$$

$$\frac{\alpha_s^b}{\alpha_s^{uds}} = 0.988 \pm 0.005\,(stat) \pm 0.004\,(syst) \pm 0.011\,(th) \tag{7}$$

It is clear from these 2 new studies that the flavour independence of α_s has been demonstrated at a level of 1% for the b quark and at a level of a few % for the c quark. Also the b mass effects in the event topology have been clearly observed at the predicted level of 5 to 8 %. The theoretical errors quoted by the 2 experiments are quite different even if they use similar theoretical assumptions and methods. Some clarifications may be needed in the future for consistent error treatment.

Assuming the flavour independence of α_s the comparison of the measured b quark mass effects with topological variables like the 3-jet rates gives a method to measure the b quark mass itself as defined in the theoretical prediction. DELPHI has already published such a measurement based on Durham jet algorithm [37]. This analysis has now been extended to the new Cambridge algorithm [38]. The analysis is not fully completed but shows already that the running mass hypothesis is still preferred. SLD has also started a measurement of the b mass using various jet algorithms and work is in progress [39].

8 4-jet production

In e^+e^- annihilation the dominant contribution to 4-jet final states on the Z pole comes from 2 classes of processes: $e^+e^- \to q\overline{q}gg$ and $e^+e^- \to q\overline{q}q\overline{q}$ where the 'three gluon vertex' contributes to the first class. The 4-jet event topology is sensitive to the relative contributions from the 2 types of processes. Using this characteristic, the colour factor ratios C_A/C_f and T_f/C_f were measured at LEP1 [40] and found to be consistent with expected QCD values within the experimental uncertainties. This result gives a clear evidence for the existence of the triple gluon vertex but no evidence for new physics, e.g. the existence of a light gluino.

Instead of measuring the relative contributions of the 2 classes an absolute measurement of the production of the 4-quark final state should be more adapted for studying the existence of light gluinos. OPAL has performed such an analysis [41] by measuring the fraction of 4 quark events (f_q) from the shape of the Bentgson-Zerwas angle (χ_{BZ}) assuming the canonical values for the colour factors given by the theory. Comparing the measured value to the O(α_s^2) prediction gives $R_{4q} = \frac{f_q^{expt.}}{f_q^{theor.}} = 2.00^{+0.32}_{-0.40}$

This apparent excess of 4-quark events measured by OPAL is consistent with QCD if one adds about 40% of unresolved 5 partons which are reconstructed as 4 jet events. These events have similar χ_{BZ} shapes but different distributions for the sum of the masses of the 2 least energetic jets compared to the QCD 4-quark events. Possible effects from other sources are not excluded but one clearly needs an O(α_s^3) calculation to improve the sensitivity.

8.1 *Gluon splitting into heavy quarks*

In e^+e^- annihilation heavy quarks are produced via two processes: the primary quark pair production and the secondary production from gluon splitting into $c\overline{c}$ or $b\overline{b}$. The latter corresponds to the 4 q process discussed previously and the limited knowledge of the gluon splitting rate into heavy quarks is the dominant theoretical uncertainty in R_b measurements.

New QCD predictions based on a resummed + $O(\alpha_s^2)$ calculation [42] exist for this process and can be compared to measurements.

The measured quantity is usually defined as $g_{Q\overline{Q}} = \frac{\sigma(Z\to q\overline{q}g, g\to Q\overline{Q})}{\sigma(Z\to hadrons)}$ where Q stands for a b or c quark. L3 has presented a new measurement of $g_{c\overline{c}}$ [43] based on the result obtained from a lepton tag analysis in 3-jet events and on the result obtained using a neural network trained to separate the gluon splitting process from the other processes using the event topology. The combined value from these 2 different analyses is $g_{c\overline{c}}$=(2.22±0.18(stat)±0.44(syst))% .

ALEPH and DELPHI have presented new measurements of $g_{b\overline{b}}$. ALEPH [44] has applied topological cuts and a lifetime tag on their 4-jet samples, tagging 2 b-jets close together and requiring a large angle between the 2 light quark jets. Figure 12 shows this angle for the various background and signal contributions. The signal is concentrated in the region above 90 degrees ($\cos(\theta_{34}) < 0$). 222 events are selected with a purity of 45% and the result is $g_{b\overline{b}}$=(2.77±0.42(stat)±0.57(syst))10^{-3}.

DELPHI [45] has extracted the multiplicity of gluon splitting into $b\overline{b}$ from the measured rate of $b\overline{b}b\overline{b}$ events in hadronic Z decays. The measured rate is $R_{4b} = \frac{Br(Z\to b\overline{b}b\overline{b})}{Br(Z\to hadrons)} = (5.4 \pm 1.8 \pm 1.5)10^{-4}$.

This measurement is done by tagging 3 b-jets in 3-jet events selected with Durham algorithm (y_{min} > 0.06). Translating this ratio into $g_{b\overline{b}}$ gives: $g_{b\overline{b}}$=(3.0±1.0(stat)±0.8(syst))10^{-3}

Combining these 3 new measurements with the previously published values of $g_{c\overline{c}}$ [46] and $g_{b\overline{b}}$ [47] allows to determine new LEP averages without theory inputs using the procedure described in Ref. 48. The preliminary values are:

$g_{c\overline{c}}$=(2.58±0.18 ±0.35)%

$g_{b\overline{b}}$=(0.273±0.038 ±0.049)%

consistent with the QCD prediction $g_{c\overline{c}}$=2.007% and $g_{b\overline{b}}$=0.175% and allowing a significant reduction of the errors on R_b from the gluon splitting process.

9 Fragmentation studies

The dynamics of hadron production can be probed using the charged particle multiplicity distribution which has been found to be very sensitive to the parameters of the QCD models. The particle distributions depend on the details of the parton shower evolution and are quite sensitive to soft gluon coherence predicted by QCD. In this regime of soft and collinear gluon emission the parton shower model as implemented in QCD models is well adapted for comparison. Figure 13 shows the evolution of mean charged particle multiplicity with centre-of-mass energy measured by various experiments[16,17,19,49,50] compared to several QCD models. The parameters of these models are the same at all energies. The energy dependence of the multiplicity distribution is in agreement with the predictions of parton shower models like JETSET, HERWIG, ARIADNE which include QCD coherence effects. However, parton shower models with no QCD coherence effects like COJETS cannot explain the energy dependence but predict a faster energy evolution. The colour coherence effect in QCD implies destructive interference in soft gluon emission. This gives rise to a suppression of hadron production at small momenta.

This effect is investigated by studying the charged particle momentum distribution in terms of the variable $\xi = \ln(1/x_p)$, where x_p is the momentum scaled by the beam energy. In the context of Local Parton Hadron Duality (LPHD) hypothesis the low energy particles produced in e^+e^- collisions are remnants of soft gluon radiation and their distributions (shapes and variations

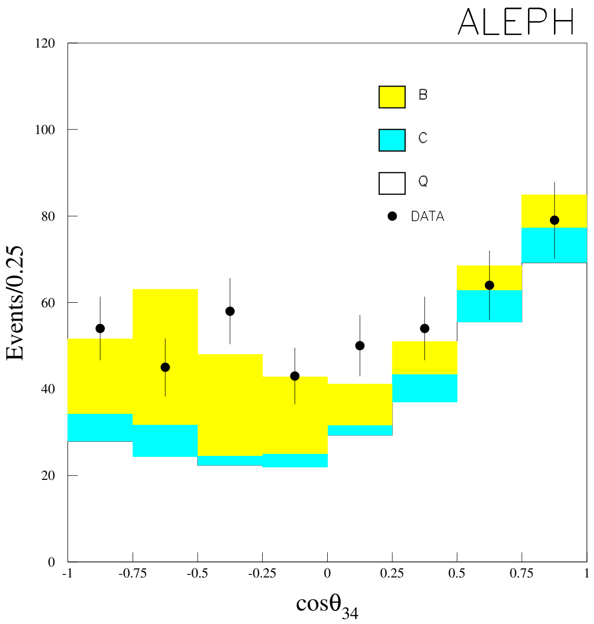

Figure 12: Angular distribution of the 2 light quark jets as measured by ALEPH together with the expected background (Q=no gluon splitting into heavy quarks, C=g → $c\overline{c}$) and the measured signal (B=g → $b\overline{b}$).

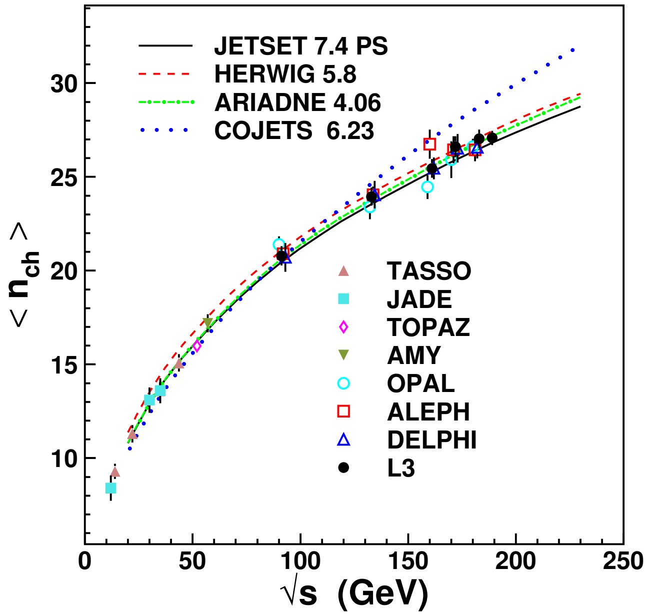

Figure 13: The mean charged particle multiplicity as a function of the e^+e^- CM energy, compared to several QCD models.

with energy) may be predicted in the framework of the Leading Logarithmic Approximation (LLA). The shape of the ξ distribution at parton level, as calculated in the Modified Leading Log Approximation (MLLA) [51], can be parametrized by a distorted gaussian [52]. In figure 14 the ξ distributions as determined from DELPHI high energy data [17] are compared to results from low energy experiments. The full lines are the results of a simultaneous fit of the Fong-Webber parametrization to the data. The distorted gaussian shape is in good agreement with the measured shape around the peak at all energies.

The effect of gluon coherence can be clearly seen with the energy evolution of the peak position of the ξ distribution ($\xi^\star$). Figure 15 shows the measured values of $\xi^\star$ as a function of centre-of-mass energy for the TASSO [53] and the LEP experiments [16,17,18,19,50,54].

The energy evolution of $\xi^\star$ has been fitted using the QCD prediction:

$$\xi^\star(s) = Y\left(\frac{1}{2} + a\sqrt{\frac{\alpha_s(Y)}{32\mathrm{N_c}\pi}} - a^2\frac{\alpha_s(Y)}{32\mathrm{N_c}\pi}\right),$$

where $Y = \ln(\sqrt{\mathrm{s}}/2\Lambda)$, $a = (11/3\mathrm{N_c}) + (2\mathrm{N_f}/3{\mathrm{N_c}}^2)$, $\mathrm{N_c}$ and $\mathrm{N_f}$ are number of colours and active flavours respectively. The first term is given by the double logarithm approximation (DLA), and the correction terms arise in the next-to-leading order (MLLA) QCD predictions.

The data are in better agreement with QCD predictions computed to the next-to-leading order. It should

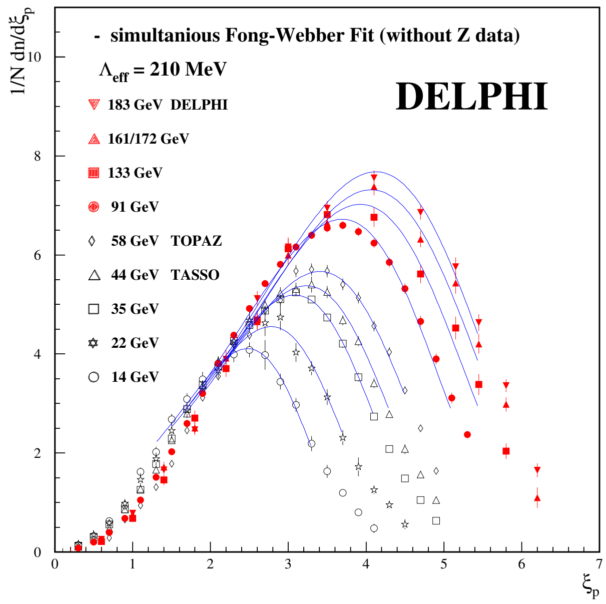

Figure 14: ξ distributions measured by DELPHI together with low energy measurements.

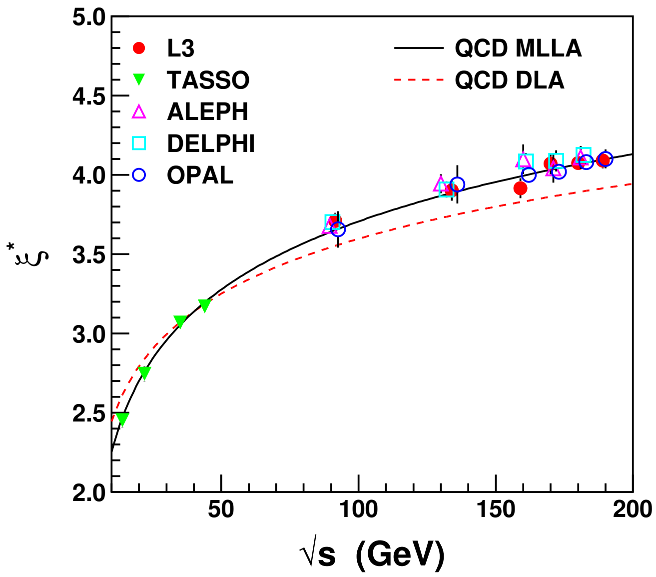

Figure 15: Energy evolution of $\xi^\star$: the solid and dashed lines are fits to the data with MLLA and DLA QCD predictions.

be recalled that the suppression of hadron production at very small momenta resulting in a bell shape of the ξ distribution is expected on purely kinematical grounds due to finite hadron masses. Soft gluon coherence, however, increases this suppression and manifests itself in the energy dependence of $\xi^{\star}$. The change with energy would be approximately two times larger without any destructive interference.

10 Quark and gluon jet properties

Differences between quark and gluon jets are expected due to their different colour charges (C_A=3 for gluon and C_f=4/3 for quark). As a consequence the gluon jets should have a larger multiplicity, should be broader and have a softer fragmentation function compared to quark jets. Naively the average charged particle multiplicity for the gluon should be larger than for the quark jet by a factor equal to the ratio of the colour charges (=9/4) [55]. From the early LEP analyses this ratio was measured to be between 1.10 and 1.25 [56]. Several attemps have been made to understand this apparent discrepancy and a lot of progress from the experimental side has been made in the recent years. It is important to recall that the QCD predictions are based on quark-antiquark and gluon-gluon colour singlet systems. Experimentally the first one is well defined while the second is not. The first studies of the differences between quark and gluon jets were done by selecting symmetric 3-jet events but the results were dependent on the jet algorithm used and the selected topologies were such that the average gluon and quark jet energy was around 24 GeV. More refined studies have been performed since then improving our understanding of the observed differences. Interesting new results have been obtained by OPAL [57] using an experimental gluon jet definition corresponding to the theoretical one [58] and by DELPHI studying the energy dependence of the quark and gluon jet properties as a function of a well adapted energy scale.

10.1 Particle multiplicity in quark and gluon jets

OPAL has studied the properties of events where a gluon recoils against 2 quarks [59]. In these events 2 b jets are tagged in the same event hemisphere and the gluon jet is defined inclusively as all the particles in the opposite hemisphere. From a study of about 3 M Z decays about 500 events are selected with a mean gluon energy of 41.6 GeV and a purity of 80%. From Monte Carlo studies it has been checked that this definition gives similar results to gluon jets produced from a color singlet source. The light quark jets are defined inclusively using the particles observed in event hemispheres opposite to those containing identified uds jets. Figure 16 shows the ra-

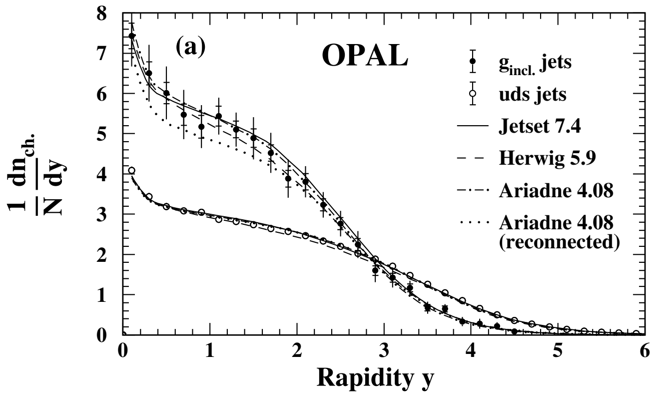

Figure 16: Charged particle rapidity distribution for 41.6 GeV gluon jets and 45 GeV quark jets.

pidity distributions of the particles in quark and gluon jets measured with respect to the sphericity axis. A factor of nearly two is observed at small rapidities between the gluon and quark jets. For $|y| < 2$ the multiplicity ratio is $r_{ch}(|y| < 2) = 1.815\pm0.038(\text{stat})\pm0.062(\text{syst})$ which is close to the QCD prediction of 2.25. Doing the measurement in a restricted rapidity interval has the advantage that energy-momentum is not locally conserved. OPAL claims that the remaining difference with the prediction comes from the finite energy available for the jet production process. The measurement of the ratio of the multiplicity between gluon and quark jet at 41.6 GeV over the full phase space gives: $r_{ch} = 1.509\pm0.022(\text{stat})\pm0.046(\text{syst})$ in agreement with analytical calculations including partial energy-momentum conservation [57].

DELPHI has investigated the scale dependence of this multiplicity ratio [60]. The ratio has been measured as a function of the "hardness" of the process. The "hardness" is defined as $\kappa = E_{jet} sin(\frac{\theta}{2})$ where E_{jet} is the jet energy and θ is the angle with respect to the closest jet. The quark and gluon jets were obtained from the 2 least energetic jets in 3-jet events clustered with Durham algorithm and y_{cut}=0.015 requiring that the angles between the low-energetic jet and the highest energetic jet be in the range 100^o to 170^o. Gluon jets were identified by anti-tagging heavy quarks and quark jets were obtained from $q\overline{q}\gamma$ or $q\overline{q}g$ events depleted from b quark and statistically subtracting identified gluon jets. The average charged particle multiplicity for gluon and quark jets are shown in figure 17(a). A stronger increase of the multiplicity with scale is observed in gluon jets compared to quark jets. This is due to the stronger gluon radiation expected from the different colour charges. The ratio r_{ch} is shown in the figure 17(b) as well as the ratio of the slope which is about 2.1 compatible with QCD expecta-

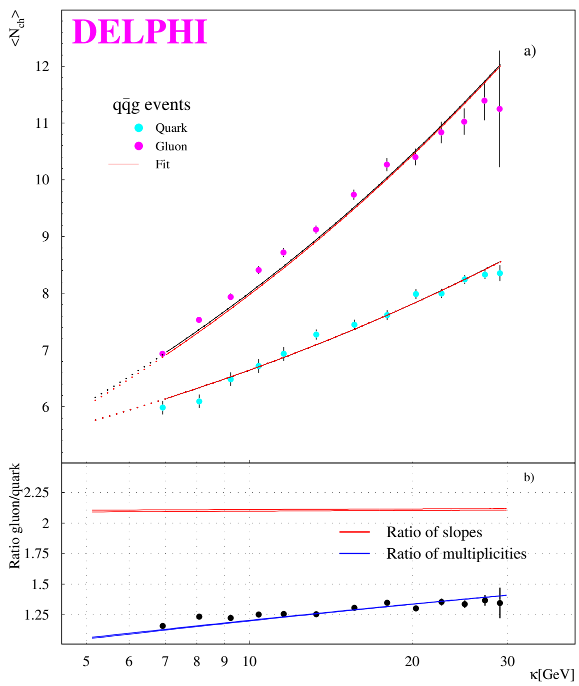

Figure 17: a) Average charged particle multiplicity for quark and gluon jets as a function of the κ scale. b) Ratio of gluon to quark multiplicity and ratio of the slopes as a function of the scale.

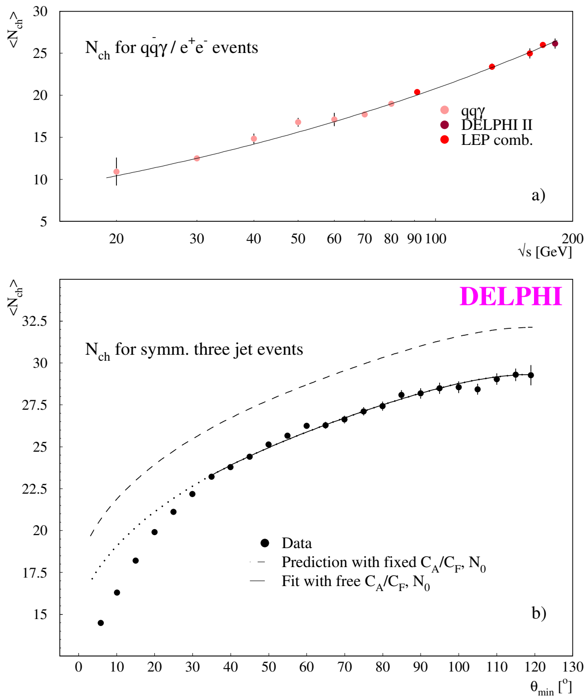

Figure 18: a) Mean charged particle multiplicity as a function of hadronic CM energy. b) Mean charged particle multiplicity in symmetric 3-jet events as a function of the opening angle. The solid line is a fit of equation 8 to the data.

tion when $C_A/C_F = 2.25$. This result gives an evidence for the triple gluon coupling based on soft gluon radiation.

The measured multiplicity ratios by OPAL at 41 GeV [59] and by CLEO [61] at a scale of about 3 GeV (r_{ch} = 1.04±0.02(stat)±0.05(syst)) agree very well with the scale dependence measured by DELPHI.

DELPHI has also investigated the scale dependence of the mean charged particle multiplicity in mirror symmetric 3-jet events (Y topology) in order to extract the ratio of the colour factors C_A/C_F [60]. The MLLA prediction for this inclusive quantity as a function of the colour factors can be written as:

$$N_{q\bar{q}g} = N_{e^+e^-}(2E^\star) + r(p_{1\perp})(\frac{1}{2}N_{e^+e^-}(p_{1\perp}) - N_0) \quad (8)$$

where r(κ) = C_A/C_F(1+higher order terms), $N_{e^+e^-}(\kappa)$ = NLO prediction for the hadron multiplicity and N_0 is a non-perturbative term added to the MLLA prediction to take into account the difference in the fragmentation of leading quarks and gluons (gluons need one further splitting to produce hadrons compared to quarks). $E^\star$ is the quark energy in the q$\bar{\text{q}}$ system centre-of-mass and $p_{1\perp}$ is the transverse momentum of the gluon. The mean multiplicity in all e^+e^- events $N_{e^+e^-}$ has been obtained from events with hard radiation for energies below the Z mass and from various LEP measurements from 91 GeV to 183 GeV and is shown in figure 18(a) as a function of the effective hadronic center of mass energy. For symmetric events the scale dependence is directly related to the opening angle between the gluon jet and the closest quark jet (θ_{min}). Figure 18(b) shows the mean multiplicity in symmetric 3-jet events as a function of the angle θ_{min}. The full line corresponds to a fit of the above prediction leaving C_A/C_F and N_0 free while the dashed line corresponds to the QCD prediction without the N_0 term. Fitting the measured multiplicity above 35^o results in:

$\frac{C_A}{C_F} = 2.266 \pm 0.053(stat) \pm 0.055(syst) \pm 0.096(theo)$ and N_0=1.43±0.09.

This is the most precise determination of C_A/C_F. The values obtained from standard 4-jet topology analyses have errors of the order of 0.2 to 0.4.

10.2 Scaling violation

DELPHI has also measured the quark and gluon fragmentation function into stable charged hadrons as a function of the scale κ [62]. Typical scaling violation behaviour is observed in gluon jets as well as in quark jets. The slopes of the scale dependence of the fragmentation functions as a function of the scaled particle momentum are

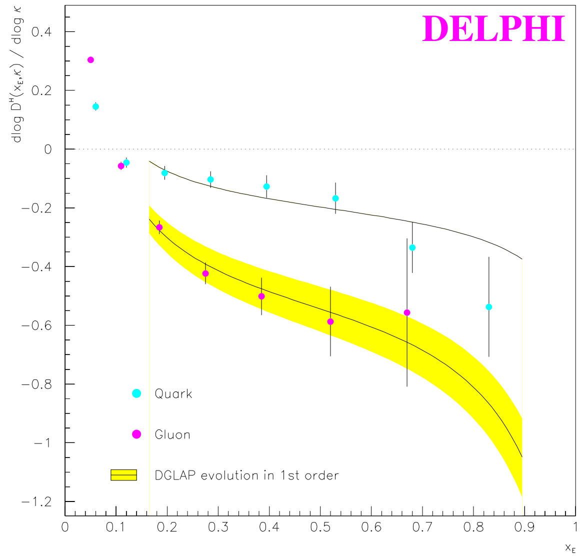

Figure 19: Comparison of scaling violations of quark and gluon jets. The solid lines are the predictions from the DGLAP evolution equations.

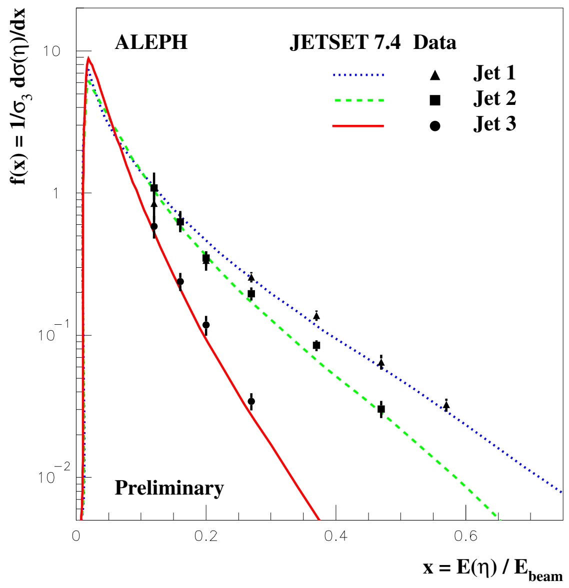

Figure 20: η fragmentation function in 3-jet events compared to JETSET prediction.

shown in figure 19 for quarks and gluons. The results are in very good agreement with the shape predicted by solving the DGLAP evolution equation at leading order using κ as the evolution variable. The scaling violations in gluon jet are observed to be much stronger than in quark jets due to the different colour charges. The value of C_A/C_F extracted from the fit of the DGLAP equations is very consistent with the previous measurement.

10.3 Identified particle rate

As discussed above the differences observed between quark and gluon jets from inclusive charged particle measurements are in good agreement with the predictions of perturbative QCD. But the theory makes no explicit predictions for the individual hadron species produced in these jets, the production mechanism relying on phenomenological models. Some QCD Monte Carlo models of hadronization predict that the relative hadron production rates in quark and gluon jets may differ for different hadron species. In the JETSET and HERWIG models the gluon fragmentation is treated similarly to quark fragmentation taking into account the different colour charges. In the independent fragmentation model of Peterson and Walsh [63] only isoscalar particles and glueballs are produced directly in the gluon fragmentation. This leads to harder spectrum for isoscalar particles in gluon jet with respect to quark jet. Identified particle production has been studied in quark and gluon jets in order to search for evidence for enhanced production of particles in gluon jets. A recent review of the few available experimental results can be found in Ref. 64. There is no clear evidence for enhanced identified isoscalar particle production in gluon as compared to quark jets from the previous studies. A L3 result [65] published 2 years ago on the observation of a harder η spectrum in gluon enriched jets than that predicted by Monte Carlo models has been the focus of some attention. At this conference ALEPH has presented a measurement of inclusive production of η and η' in two and three jet events [66]. Figure 20 shows the measured η fragmentation function in three-jet events compared to JETSET prediction. The data are in very good agreement with the Monte Carlo prediction especially in the third jet representing the gluon jet more than 70% of the cases. The same remark holds for the η' fragmentation function in three-jet events shown in figure 21. ALEPH sees no experimental evidence for enhanced isoscalar meson production in gluon jets with respect to quark jets within the errors. The difference with the L3 results seems to come only from the Monte Carlo prediction used to do the comparison. The data results are consistent between the 2 experiments.

Two new contributions on the production of K^0_s and Λ production in quark and gluon jets from ALEPH [67] and OPAL [68] have been shown at this conference. ALEPH has compared directly the content of K^0_s and Λ in the jets of two- and three-jet events to model predictions. They have found a reasonable agreement of the momentum spectra of the studied strange hadrons with JETSET prediction but poor results with the HERWIG model. OPAL

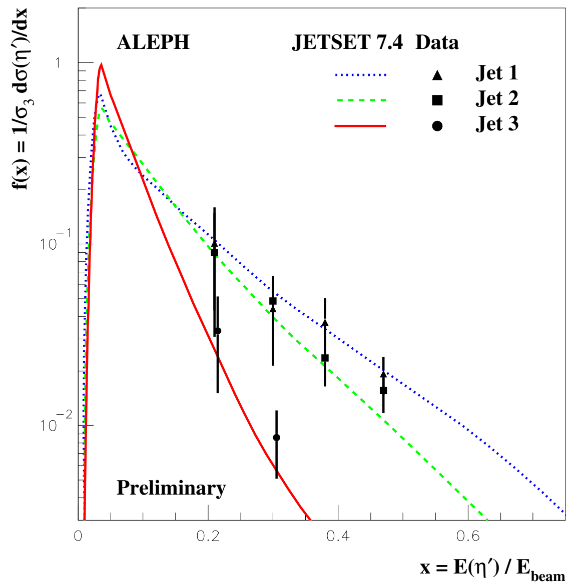

Figure 21: η' fragmentation function in 3-jet events compared to JETSET prediction.

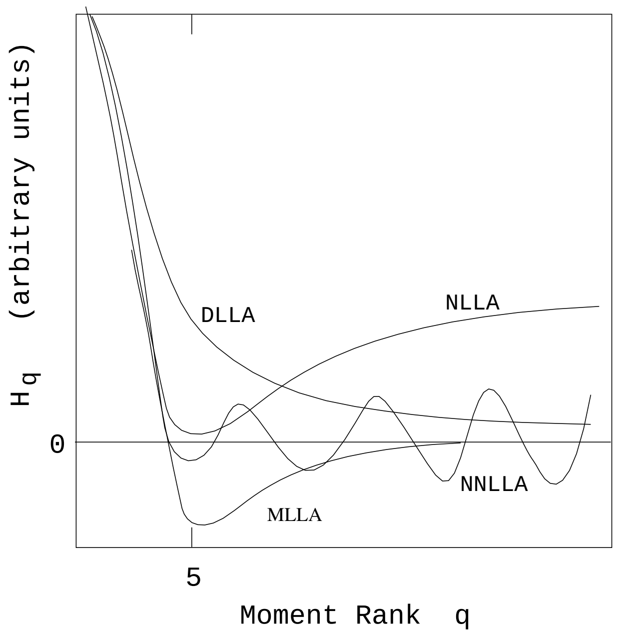

Figure 22: Different perturbative QCD predictions for H_q as a function of the rank q.

has investigated the production rate of these particles using 2 different approaches. As a result an enhancement of Λ production in gluon jets relative to quark jets in excess of that for charged particles is observed but is consistent with the JETSET prediction. The smaller enhancement observed for K_s^0 is also consistent with JETSET. HERWIG fails to provide a good description of the OPAL data.

OPAL has also shown a study of the production rate of charged particles ($\pi^{\pm}$, $K^{\pm}$, and p($\overline{p}$)) [69]. Charged pions and protons seem to be more frequently produced in gluon jets, while charged kaons are produced more often in quark jets. This is in qualitative agreement with JETSET.

11 Hadronization

11.1 *Particle production*

A large amount of work has been done in the field of inclusive production of identified particles in the recent years by SLD and LEP experiments to improve our knowledge of the hadronization process. At this conference new measurements of the production in hadronic Z decays of more than 20 particles have been reported. These are: $\pi^{\pm}$, $K^{\pm}$, $p/\overline{p}$, $\Lambda/\overline{\Lambda}$, ϕ,γ, π^0, η, ω, η',$a_0^{\pm}$, ρ, $f_0(980)$, $f_2(1270)$, $K_2^{\star}(1430)$, f_2' and $\phi(1020)$.

It includes three new results relative to PDG98 content [70] which are the production rate per hadronic Z decay of $a_0^{\pm}$ measured for the first time by OPAL [71], $f_0(980)$ and $f_2(1270)$ measured by OPAL [72] and DELPHI [73].

A detailed review of the new results can be found in Ref. 74.

11.2 *Particle correlations*

Another field of research which gives additional information on the hadronization mechanism is the world of multiplicity fluctuations and multiparticle correlations. At this conference five contributions on this topic in e^+e^- have been submitted. Local multiplicity fluctuations have been studied using factorial and cumulant moments by L3 [75] and OPAL [76]. The data are in good agreement with the JETSET and HERWIG Monte Carlo models for these observables. L3 has performed a study of the fluctuations by using "Bunching parameters" [77] which have some advantages. DELPHI has studied angular correlations between 2 particles [78]. Again a good agreement was found with JETSET Monte Carlo but not with asymptotic QCD prediction assuming LPHD. Some disagreement with perturbative QCD predictions and LPHD was also discussed in a L3 paper concerning angular multiplicity fluctuations [79]. A more detailed review of these results can be found in Ref. 80.

An interesting result concerns the ratio of cumulant to factorial moments, H_q, measured by L3 from the multiplicity distribution in full phase space [81]. The ratio H_q is calculable in higher order perturbative QCD for soft gluons and assuming LPHD the calculation should also be valid for the ratio obtained from the charged parti-

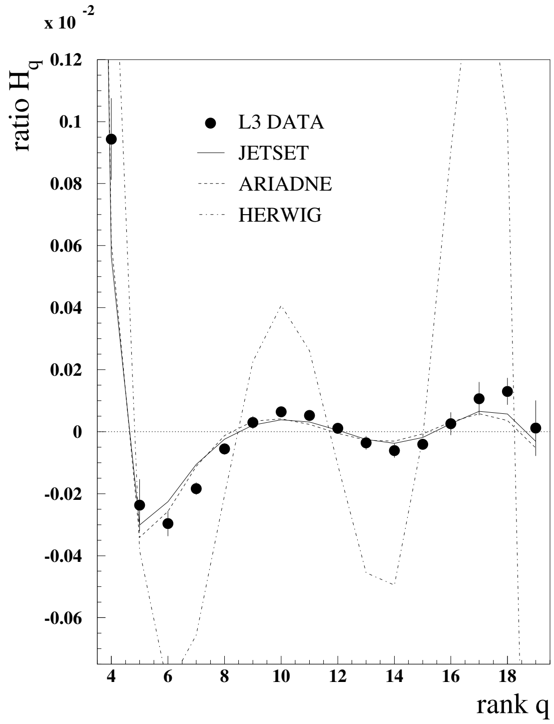

Figure 23: Measured H_q as a function of the rank q compared to QCD model predictions. The errors include both statistical and systematic contributions.

cle distribution. The predicted distribution is shown on figure 22 as a function of the rank q for various theoretical approximations. The same quantity as measured by L3 is shown in figure 23 together with JETSET and HERWIG prediction. A clear oscillatory behaviour reproduced by the Monte Carlo models (only qualitatively by HERWIG) is seen. This is in agreement with the same measurement done by SLD two years ago [82]. The MLLA prediction does not show any oscillation while surprisingly models which are based on a similar approximation (NLLA) do show this behaviour. This effect is probably associated with non-perturbative phase and MLLA prediction assuming LPHD cannot predict the observed oscillation. For this type of observables more precise calculations are needed.

Comment

As can be seen from this review a lot of recent studies of QCD in e^+e^- collisions have been performed. Unfortunately it was not possible to cover all the very interesting results which were presented and discussed during the parallel sessions. I would also like to apologize for omitting the results on fragmentation functions and on the new studies of the structure of $b\bar{b}g$ events. The reader interested in these two topics is referred to the reports written by M. Hapke [83] and D. Muller [84] in these proceedings.

12 Summary

The main achievements from recent studies of $e^+e^- \longrightarrow$ hadrons include several precise tests of the theory of the strong interaction.

The large amount of data collected at the Z pole at the SLD and LEP colliders has allowed very accurate determination of the strong coupling constant, α_s, as well as demonstration of the flavour independence of α_s at a few percent level. This was possible with the introduction of new complete QCD calculations including heavy quark mass effects. The uncertainty on the determination of α_s from event shape distributions is completely dominated by theoretical errors. The error treatment which has been somewhat conservative up to now should probably be reconsidered to avoid possible overestimation. Also new theoretical approaches, for example the power correction calculations, should also be fully exploited.

The experiments have developed very efficient analysis techniques for detailed flavour dependent QCD studies. The process of gluon splitting into $c\bar{c}$ and $b\bar{b}$ has been investigated and measured with improved precision reducing significantly the theoretical error of R_b measurements.

The results obtained on the study of quark and gluon jet properties and their differences are impressive. Many of the measurements confirm the predicted differences and are used now to test theoretical predictions with a good accuracy.

On the hadronization side there are a lot of comprehensive studies for particle production and correlations with improved results.

The high energies available at LEP2 have allowed the study of the global event properties over a wide energy range (14 GeV $< \sqrt{s} <$ 189 GeV) and the test of QCD model predictions which include gluon coherence and higher order QCD effects.

The energy evolution of α_s has been measured from 91 to 189 GeV and shows no deviation with the evolution predicted by QCD within the experimental uncertainties. The measurement of inclusive particle distributions at LEP2 gives a clean evidence for soft gluon coherence.

In conclusion we can say that QCD still proves to be a very consistent theory to describe many aspects of jet dynamics and properties in e^+e^- annihilations.

Acknowledgements

Preparing such a review needs a lot of discussion and interaction with many people. For this reason and much more I would like to thank Glen Cowan, Klaus Hamacher, Jürgen Drees, Juan Fuster, John Field, Wes Metzger, Siggi Bethke, Stan Bentvelsen, Jules Gascon, Philip Burrows from ALEPH, DELPHI, L3, OPAL and SLD for their great help in preparing this talk and the numerous interesting discussions we exchanged during that period.

References

1. G. Hanson et *et al.*, Phys. Rev. Lett. **35** (1975) 1609.
2. TASSO Collaboration, R. Brandelik *et al.*, Phys. Lett. **B86** (1979) 243.
3. S. Bethke, Nucl. Phys. B (proc. suppl.) **64** (1998) 54.
4. P. Mättig, Phys. Rep. **177** (1989) 141;
T. Hebbeker, Phys. Rep. **217** (1992) 69;
S. Bethke and J.E. Pilcher, Ann. Rev. Nucl. Part. Sci. **42** (1992) 251;
M. Schmelling, Phys. Scr. **51** (1995) 683;
P.N. Burrows, proc. of XXIV SLAC Summer Institute on Particle Physics (1996) 101.
5. Z. Kunszt and P. Nason, Z physics at LEP1, CERN89-08 **Vol. I** (1989) 373.
6. S. Catani and M.H. Seymour, Phys. Lett. **B378** (1996) 287; Nucl. Phys. **B485** (1997) 291.
7. G. Rodrigo and A. Santamaria, Phys. Rev. Lett. **79** (1997) 193.
8. W. Bernreuther, A. Brandenburg and P. Uwer, Phys. Rev. Lett. **79** (1997) 189.
9. P. Nason and C. Oleari, Phys. Lett. **B407** (1997) 57.
10. S. Catani *et al.*, Phys. Lett. **B263** (1991) 491;
S. Catani *et al.*, Phys. Lett. **B269** (1991) 432;
S. Catani, G. Turnock and B.R. Webber, Phys. Lett. **B272** (1991) 368; Phys. Lett. **B295** (1992) 269;
S. Bethke *et al.*, Nucl. Phys. **B370** (1992) 310;
S. Catani *et al.*, Nucl. Phys. **B407** (1993) 3;
G. Dissertori and M. Schmelling, Phys. Lett. **B361** (1995) 167;
S. Catani and B.R. Webber, Phys. Lett. **B427** (1998) 377.
11. A. Signer and L. Dixon, Phys. Rev. Lett. **78** (1997) 811.
12. G. Altarelli and G. Parisi, Nucl. Phys. **B126** (1977) 298;
Yu. L. Dokshitzer, Sov. Phys. JETP **46** (1977) 641;
Yu.L. Dokshitzer *et al.*, Basics of Perturbative QCD, Editions Frontieres, Gif-sur-Yvette, 1991.
13. Yu.L. Dokshitzer and B.R. Webber, Phys. Lett. **B352** (1995) 451; Cavendish HEP-97-2 (1997).
14. Ya.I. Azimov *et al.*,Z. Phys. **C27** (1985) 65.
15. ALEPH Collaboration, R. Barate *et al.*, Phys. Rep. **294** (1998) 1;
DELPHI Collaboration, P. Abreu *et al.*, Z. Phys. **C73** (1996) 11;
L3 Collaboration, B. Adeva *et al.*, Z. Phys. **C55** (1992) 39; L3 note 1978 (1996);
OPAL Collaboration, G. Alexander *et al.*, Z. Phys. **C69** (1996) 543.
16. ALEPH Collaboration, ICHEP'98 contributed paper #945.
17. DELPHI Collaboration, ICHEP'98 contributed paper #138.
18. L3 Collaboration, ICHEP'98 contributed paper #536 and references therein.
19. OPAL Collaboration, ICHEP'98 contributed paper #304.
20. Yu.L. Dokshitzer *et al.*, JHEP **08** (1997) 1.
21. S. Bentvelsen and I. Meyer , Eur. Phys. J. **C4** (1998) 623.
22. S.G. Gorishny, A.L. Kataev and S.A. Larin, Phys. Lett. **B259** (1991) 144;
L.R. Surguladze and M.A. Samuel, Phys. Rev. Lett. **66** (1991) 560.
23. E. Braaten, S. Narison and A. Pich, Nucl. Phys. **B373** (1992) 581;
F. Le Diberder and A. Pich, Phys. Lett. **B289** (1992) 165.
24. DELPHI Collaboration, ICHEP'98 contributed paper #142.
25. P.M. Stevenson, Phys. Rev. **D23** (1981) 2916;
G. Grunberg, Phys. Rev. **D29** (1984) 2315;
S.J. Brodsky, G.P. Lepage and P.B. Mackenzie, Phys. Rev. **D28** (1983) 228.
26. S. Bethke, Z. Phys. **C43** (1989) 331.
27. ALEPH Collaboration, ICHEP'98 contributed paper #940.
28. DELPHI Collaboration, ICHEP'98 contributed paper #137.
29. P.A. Movilla-Fernández, O. Biebel and S. Bethke, ICHEP'98 contributed paper #646.
30. D. Karlen, these proceedings.
31. ALEPH Collaboration, R. Barate *et al.*, Eur. Phys. J. **C4** (1998) 409.
32. OPAL Collaboration, K. Ackerstaff *et al.*, CERN-EP/98-102 (1998).
33. S. Bethke, private communication.
34. Yu.L. Dokshitzer , these proceedings.
35. SLD Collaboration, ICHEP'98 contributed paper #253.
36. OPAL Collaboration, ICHEP'98 contributed paper #295.
37. DELPHI Collaboration, P. Abreu *et al.*, Phys. Lett. **B418** (1998) 430.

38. DELPHI Collaboration, ICHEP'98 contributed paper #152.
39. P.N. Burrows , these proceedings.
40. ALEPH Collaboration, D. Decamp *et al.*, Phys. Lett. **B284** (1992) 151; ALEPH Collaboration, R. Barate *et al.*, Z. Phys. **C76** (1997) 1;
DELPHI Collaboration, P. Abreu *et al.*, Z. Phys. **C59** (1993) 357;
OPAL Collaboration, R. Akers *et al.*, Z. Phys. **C65** (1995) 367.
41. OPAL Collaboration, ICHEP'98 contributed paper #293.
42. M.H. Seymour, Nucl. Phys. **B436** (1995) 163;
D.J. Miller and M.H. Seymour, RAL-TR98-042, hep-ph/9805414 (1998).
43. L3 Collaboration, ICHEP'98 contributed paper #539.
44. ALEPH Collaboration, R. Barate *et al.*, CERN-EP/98-103 (1998).
45. DELPHI Collaboration, ICHEP'98 contributed paper #776.
46. OPAL Collaboration, R. Akers *et al.*, Phys. Lett. **B353** (1995) 595; Z. Phys. **C67** (1995) 27.
47. DELPHI Collaboration, P. Abreu *et al.*, Phys. Lett. **B405** (1997) 202.
48. C. Paus , these proceedings.
49. L3 Collaboration, ICHEP'98 contributed paper #536 and references therein.
50. L3 Collaboration, ICHEP'98 contributed paper #484.
51. Yu.L. Dokshitzer *et al.*, Basics of Perturbative QCD, Editions Frontieres, Gif-sur-Yvette, 1991.
52. C.P. Fong and B.R. Webber, Phys. Lett. **B229** (1989) 289.
53. TASSO Collaboration, W. Braunschweig *et al.*, Z. Phys. **C47** (1990) 187.
54. OPAL Collaboration, ICHEP'98 contributed paper #1067.
55. S.J. Brodsky and J.F. Gunion, Phys. Rev. Lett. **37** (1976) 402.
56. ALEPH Collaboration, D. Buskulic *et al.*, Phys. Lett. **B384** (1996) 353;
DELPHI Collaboration, P. Abreu *et al.*, Z. Phys. **C70** (1996) 179;
OPAL Collaboration, R. Akers *et al.*, Z. Phys. **C68** (1995) 179.
57. OPAL Collaboration, G. Alexander *et al.*, Phys. Lett. **B388** (1996) 659; OPAL Collaboration, K. Ackerstaff *et al.*, Eur. Phys J. **C1** (1998) 479.
58. J.W. Gary, Phys. Rev. **D49** (1994) 4503.
59. OPAL Collaboration, ICHEP'98 contributed paper #296.
60. DELPHI Collaboration, ICHEP'98 contributed paper #146.
61. CLEO Collaboration, M.S. Alam *et al.*, Phys. Rev. **D56** (1997) 17.
62. DELPHI Collaboration, ICHEP'98 contributed paper #147.
63. C. Peterson and T.F. Walsh, Phys. Lett. **B91** (1980) 455.
64. I.G. Knowles and G.D. Lafferty, J. Phys. **G23** (1997) 731.
65. L3 Collaboration, M. Acciarri *et al.*, Phys. Lett. **B371** (1996) 126.
66. ALEPH Collaboration, ICHEP'98 contributed paper #934.
67. ALEPH Collaboration, ICHEP'98 contributed paper #935.
68. OPAL Collaboration, K. Ackerstaff *et al.*, CERN-EP/98-058 (1998).
69. OPAL Collaboration, ICHEP'98 contributed paper #388.
70. Particle Data Group, C. Caso *et al.*, Eur. Phys. J. **C3** (1998) 1.
71. OPAL Collaboration, K. Ackerstaff *et al.*, CERN-EP/98-054 (1998).
72. OPAL Collaboration, K. Ackerstaff *et al.*, CERN-EP/98-010 (1998).
73. DELPHI Collaboration, ICHEP'98 contributed paper #144.
74. P. Abreu, these proceedings.
75. L3 Collaboration, M. Acciarri *et al.*, Phys. Lett. **B429** (1998) 375.
76. OPAL Collaboration, ICHEP'98 contributed paper #297.
77. S.V. Chekanov and V.I. Kuvshinov, Acta Phys. Polonica **B25** (1994) 1189;
S.V. Chekanov, W. Kittel and V.I. Kuvshinov, Acta Phys. Polonica **B27** (1996) 1739. S.V. Chekanov, W. Kittel and V.I. Kuvshinov, Z. Phys. **C74** (1997) 517.
78. DELPHI Collaboration, ICHEP'98 contributed paper #149.
79. L3 Collaboration, M. Acciarri *et al.*, Phys. Lett. **B428** (1998) 186.
80. W. Metzger, these proceedings.
81. L3 Collaboration, ICHEP'98 contributed paper #541.
82. SLD Collaboration, K. Abe *et al.*, Phys. Lett. **B371** (1996) 149.
83. M. Hapke, these proceedings.
84. D. Muller, these proceedings.